Crystallization of Aqueous Ammonium Sulfate Particles Internally Mixed with Soot and Kaolinite: Crystallization Relative Humidities and Nucleation Rates

Atul Pant, Matthew T. Parsons, and Allan K. Bertram*

Department of Chemistry, University of British Columbia, 2036 Main Mall, Vancouver, BC, Canada V6T 1Z1

Received: February 15, 2006; In Final Form: May 15, 2006

Using optical microscopy, we investigated the crystallization of aqueous ammonium sulfate droplets containing soot and kaolinite, as well as the crystallization of aqueous ammonium sulfate droplets free of solid material. Our results show that soot did not influence the crystallization RH of aqueous ammonium sulfate particles under our experimental conditions. In contrast, kaolinite increased the crystallization RH of the aqueous ammonium sulfate droplets by approximately 10%. In addition, our results show that the crystallization RH of aqueous ammonium sulfate droplets free of solid material does not depend strongly on particle size. This is consistent with conclusions made previously in the literature, based on comparisons of results from different laboratories. From the crystallization results we determined the homogeneous nucleation rates of crystalline ammonium sulfate in aqueous ammonium sulfate droplets and the heterogeneous nucleation rates of crystalline ammonium sulfate in aqueous ammonium sulfate particles containing kaolinite. Using classical nucleation theory and our experimental data, we determined that the interfacial tension between an ammonium sulfate critical nucleus and an aqueous ammonium sulfate solution is 0.064 ± 0.003 J m^{-2} (in agreement with our previous measurements), and the contact angle between an ammonium sulfate critical nucleus and a kaolinite surface is $59 \pm 2°$. On the basis of our results, we argue that soot will not influence the crystallization RH of aqueous ammonium sulfate droplets in the atmosphere, but kaolinite can significantly modify the crystallization RH of atmospheric ammonium sulfate droplets. As an example, the CRH50 (the relative humidity at which 50% of the droplets crystallize) ranges from about 41 to 51% RH when the diameter of the kaolinite inclusion ranges from 0.1 to 5 μm. For comparison, the CRH50 of aqueous ammonium sulfate droplets (0.5 μm diameter) free of solid material is approximately 34.3% RH under atmospheric conditions.

1. Introduction

Aerosol particles are abundant in the atmosphere, and these particles can undergo several types of phase transitions. An example of an atmospherically relevant phase transition is crystallization, which here refers to the crystallization of a solute in an aqueous solution droplet at low values of relative humidity (in this case water is considered the solvent). An example of crystallization includes the precipitation of crystalline ammonium sulfate in an aqueous ammonium sulfate droplet at low values of relative humidity. This last process is also often called efflorescence. Crystallization is a kinetically controlled process due to the free energy barrier associated with nucleation of a crystalline solid in an aqueous solution. As a result, crystallization of aqueous particles typically does not occur at the same relative humidity (RH) as deliquescence, which refers to when particles take up water to form solution droplets. In the absence of heterogeneous nuclei, crystallization occurs by homogeneous nucleation; otherwise, crystallization can occur by heterogeneous nucleation.

Knowledge of the conditions required for crystallization of atmospheric aqueous particles is necessary to predict if particles in the atmosphere are solid, liquid, or mixtures of solid and liquid. This information is, in turn, necessary to predict the rates of heterogeneous reactions occurring on and in particles, the amount of light particles scatter and absorb, and their ability to act as ice nuclei.[1−4]

* To whom correspondence should be addressed. E-mail: bertram@chem.ubc.ca.

Field measurements have shown that a majority of the fine particulate mass (less than 2 μm in diameter) in the troposphere consists of sulfate, ammonium, and nitrate ions, as well as organic material.[5] The crystallization of aqueous inorganic particles, such as aqueous $(NH_4)_2SO_4$ particles, has been studied extensively in the past (see for example ref 2 and references therein). More recently, researchers have started to study the crystallization of aqueous organic and aqueous organic−inorganic particles due to the atmospheric abundance of these types of particles (see for example refs 6−16 and references therein). Aqueous particles in the atmosphere may also contain solid material, such as soot and mineral dust, which could lower the free energy barrier to nucleation of crystalline material and, hence, change the crystallization RH of the aqueous particles. In this case, the particles can crystallize by heterogeneous nucleation in addition to homogeneous nucleation. See refs 11 and 17−24 for studies on crystallization of aqueous particles containing heterogeneous nuclei relevant for the atmosphere.

There is now evidence that a large fraction of sulfate particles in the troposphere contain soot material (i.e., sulfate and soot are often internally mixed).[25−28] For example, Pósfai et al.[27] found that in the polluted north Atlantic marine boundary layer about 50% of the smallest and 90% of the larger (approximately 1 μm in diameter) sulfate particles contained soot. They concluded that internally mixed soot and sulfate appear to comprise a globally significant fraction of aerosols in the troposphere. Two recent studies have investigated the effect of soot and carbon black on the crystallization of aqueous inorganic

10.1021/jp060985s CCC: $33.50
Published on Web 06/17/2006

particles. Dougle et al.[17] found that the addition of soot from the combustion of diesel fuel did not modify the crystallization RH of aqueous ammonium nitrate particles or aqueous particles consisting of 2:1 internal mixtures by weight of ammonium nitrate to ammonium sulfate, and Even et al.[18] found that Talens Indian ink (a type of carbon black) did not modify the crystallization RH of aqueous sodium chloride particles. However, the studies by Dougle et al.[17] and Even et al.[18] only investigated two types of soot and a limited number of solution compositions. More studies similar to those by Dougle et al.[17] and Even et al.[18] are still needed to establish categorically that soot does not modify the crystallization RH of aqueous inorganic particles relevant for the atmosphere. First, studies need to be carried out with different types of soot. Soot in the atmosphere may have a range of properties (size, chemical composition, porosity, etc.) depending on the source. Some types of soot may be good heterogeneous nuclei for crystallization and other types of soot may not. Second, studies of other atmospherically relevant aqueous compositions would be beneficial, as soot may influence the crystallization of some inorganic salts but not others.

There is also abundant evidence that mineral dust particles can be internally mixed with sulfate and nitrate.[25,26,29−33] For example, Liu et al.[32] and Lee et al.[26] found that mineral dust particles in the Atlanta region often contain sulfate and nitrate indicating aged dust. Recent studies suggest that components of mineral dust can lower the free energy barrier to nucleation of crystalline material and, hence, modify the RH at which aqueous inorganic particles crystallize.[19−23] Nevertheless, more work in this area is needed to fully quantify the effect of mineral dust on crystallization of aqueous droplets in the atmosphere. For example, the crystallization of aqueous droplets in the presence of kaolinite, illite, and montmorillonite, which are major components of mineral dust,[34,35] has not been investigated.

Mineral dust particles are abundant in the atmosphere. This dust is largely produced from the Gobi and Saharan deserts[36,37] then transported over long distances becoming coated with sulfates and other electrolytes.[38] These mineral dust particles are believed to have a significant effect on the Earth's radiation budget by absorbing and scattering solar and infrared radiation. Dust particles and dust particles coated with sulfates can also indirectly affect climate by acting as ice nuclei.[39,40] Furthermore, modeling studies have suggested that these mineral dust particles can modify the oxidative capacity of the atmosphere.[41] To better understand the role of mineral dust in the atmosphere, knowledge of the hygroscopic properties (including crystallization) of dust particles coated with sulfates would be beneficial.

In the following, we use optical microscopy to investigate the crystallization of aqueous ammonium sulfate droplets containing soot and kaolinite. For comparison purposes we also investigated the crystallization of aqueous ammonium sulfate droplets free of solid material. We determined the range over which crystallization occurred and the RH at which 50% of the particles crystallized as a function of droplet size for aqueous ammonium sulfate droplets and aqueous ammonium sulfate droplets internally mixed with kaolinite or soot. In addition, we determined the homogeneous nucleation rates (number of nucleation events per unit volume of the aqueous droplet per unit time) of crystalline ammonium sulfate in aqueous ammonium sulfate droplets free of solid material and the heterogeneous nucleation rates (number of nucleation events per unit surface area of solid material per unit time) of crystalline ammonium sulfate in aqueous ammonium sulfate droplets containing kaolinite. We also parametrized the homogeneous and heterogeneous nucleation rates using classical nucleation theory. In this analysis, we determined the interfacial tension between a crystalline ammonium sulfate critical nucleus and an aqueous solution of ammonium sulfate and the contact angle between a solid ammonium sulfate critical nucleus and a kaolinite surface. From the combined results, we discuss if soot or kaolinite can modify the crystallization RH of aqueous ammonium sulfate droplets in the atmosphere. This combined analysis provides insight into the kinetics of nucleation in aqueous solutions in addition to crystallization of aqueous droplets in the atmosphere.

TABLE 1: Properties of Soot and Kaolinite Particles Used in These Experiments

solid inclusion	BET surface area ($m^2\ g^{-1}$)	average primary particle size (μm)
n-hexane soot (diffusion flame)	89 ± 2[a]	0.05−0.1 (spheroids)[a]
n-hexane soot (air:fuel = 0.53)	100 ± 2[b]	0.05−0.1 (spheroids)[b]
n-hexane soot (air:fuel = 2.4)	156 ± 11[b]	0.05−0.1 (spheroids)[b]
kaolinite	∼9[c]	∼2.1[c]

[a] Akhter et al.[45] [b] Chughtai et al.[44] [c] From vendor.

2. Experimental Section

The apparatus consisted of an optical microscope coupled to a flow cell.[14,15,42,43] The apparatus used in this study is similar to the apparatus we used previously to measure crystallization and deliquescence of organic and mixed organic−inorganic particles,[14,15,43] except that images of the particles recorded during the crystallization experiments were analyzed with digital analysis software in the current study. This allowed us to routinely monitor the phase and size of many individual particles during the crystallization experiments. The particles of interest (aqueous ammonium sulfate droplets with or without solid material, depending on the experiment) were deposited on the bottom surface of the flow cell and monitored with the optical microscope (using polarized light). For the experiments involving aqueous droplets without solid material, droplets with diameters ranging from 5 to 30 μm were investigated. For the experiments involving aqueous droplets with solid inclusions, only droplets with diameters ranging from 10 to 30 μm were investigated to ensure the droplets were significantly larger than the size of the solid inclusions. The bottom surface of the flow cell, which supported the particles, consisted of a hydrophobic poly(tetrafluoroethylene) (PTFE) film annealed to a glass cover slide. RH over the particles was controlled by a continuous flow of a mixture of dry and humidified N_2 gas. RH uncertainty for individual measurements was about ±1% RH based on the accuracy of the RH monitoring equipment.

Three different samples of *n*-hexane soot were used in these studies (provided by D. M. Smith, University of Denver). The first sample was produced by burning *n*-hexane under ambient conditions in an open vessel, resulting in a diffusion flame. The second and third samples were generated using an apparatus designed for producing premixed flames with variable air-to-fuel ratios. Previous measurements have shown that there is a linear relationship between the state of soot surface oxidation and the air-to-fuel ratio.[44] Properties of *n*-hexane soot have been documented by Smith and co-workers.[44,45] The kaolinite particles used in our experiments were purchased from Fluka Chemika (purum; natural grade). Listed in Table 1 is the Brunauer, Emmett, and Teller (BET) surface area per unit mass and average primary particle size of the solid materials investigated.

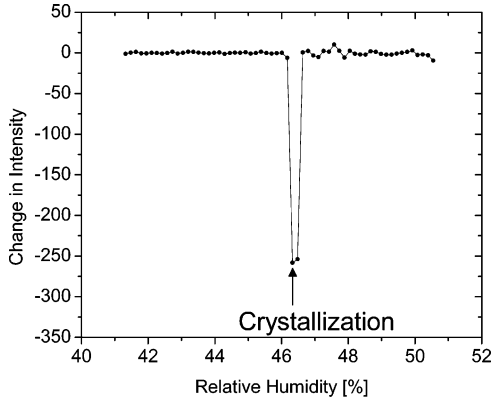

Figure 1. Change in the intensity of the light reflected by a single aqueous ammonium sulfate droplet containing kaolinite as a function of RH during a crystallization experiment. At 46.3% RH, the change in intensity deviates significantly from zero, indicating that the droplet crystallized.

Aqueous ammonium sulfate droplets internally mixed with solid material were prepared by first making a solution of 10 g L^{-1} ammonium sulfate in water. 18.2 MΩ water from a Millipore Simplicity 185 water purification system was used to make the solutions. The aqueous solutions were mixed with *n*-hexane soot or kaolinite and then placed in an ultrasonic bath for ∼30 min to make a stable suspension. In all cases the mass ratio of soot or kaolinite to ammonium sulfate was 0.01. Aqueous droplets containing solid material were created by passing these suspensions through a concentric flow pneumatic nebulizer that had a large liquid capillary opening to avoid plugging of the nebulizer by the solid material. Droplets from the nebulizer were directed to the bottom surface of the flow cell where they impacted on the PTFE surface and coagulated to form supermicrometer droplets. The contact angle between aqueous ammonium sulfate droplets and aqueous droplets containing solid material on the PTFE surface was close to 120°. In our experiments, we could not measure precisely the size of the inclusions in individual droplets. We assumed that the kaolinite and the soot particles were randomly distributed in the droplets in the same proportion as in the bulk solutions.

We verified that each droplet contained solid material in the soot and kaolinite experiments by monitoring individual droplets with a 50× objective lens. It was clear from these tests that all aqueous ammonium sulfate droplets investigated contained solid particulates, and the solid was present both within the bulk and close to the interface of the aqueous ammonium sulfate droplets. The solid particulates within the bulk of the droplets moved in all directions whereas solid particulates near the interface of the droplets moved along the interface of the droplets. This movement is likely from Brownian motion.

During a crystallization experiment the flow cell was maintained at a temperature of 293.2 ± 0.1 K and the RH was decreased at a rate of 0.5% $minute^{-1}$. The RH was monitored with a dew point hygrometer. Images of the particles were recorded every 15 s with a corresponding dew point measurement (from the hygrometer). From the images, the size of each droplet and also the RH at which each droplet crystallized was determined with image analysis software (Northern Eclipse). The crystallization RH of the droplets could be clearly determined from the images as crystallized particles appear very bright under polarized light. Shown in Figure 1 is a plot of the change of the intensity of the light reflected by a single aqueous ammonium sulfate droplet with kaolinite during a crystallization experiment determined with the image analysis software. The change in intensity was calculated by taking the derivative of the intensity with respect to RH. At 46.3% RH, the change in intensity deviates significantly from zero, indicating that the droplet had crystallized. From plots similar to Figure 1, we determined the crystallization RH of each droplet.

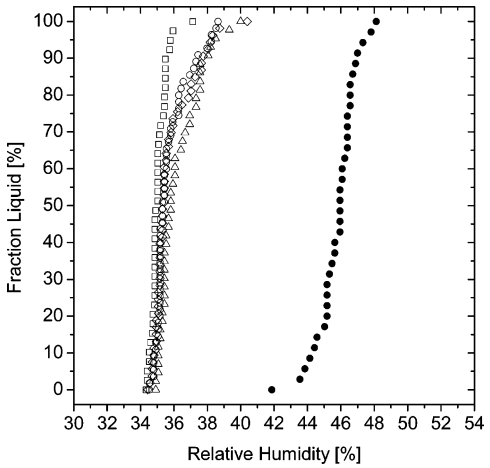

Figure 2. Examples of results from typical RH cycles (i.e., experimental runs). Each data set corresponds to a single RH cycle, and each data point corresponds to a single crystallization event. During the experiments the relative humidity was decreased at a rate of 0.5% RH $minute^{-1}$. Key: (□) aqueous ammonium sulfate; aqueous ammonium sulfate internally mixed with (○) *n*-hexane soot (diffusion flame), (◇) *n*-hexane soot (air:fuel = 0.53), (△) *n*-hexane soot (air:fuel = 2.4), and (●) kaolinite. The solid inclusion to ammonium sulfate mass ratio was 0.01 in these experiments.

3. Results and Discussions

3.1. Crystallization of Aqueous Ammonium Sulfate Droplets and Droplets Containing Soot or Kaolinite. Shown in Figure 2 are examples of results from typical RH cycles (i.e., experimental runs). Each data set corresponds to a single RH cycle, and each data point corresponds to a single crystallization event. This figure is included to illustrate the type of results obtained in an RH cycle, and it should not be used exclusively to compare the crystallization of different droplet types, since it does not take into account the fact that different droplet sizes were often used in the different RH cycles.

For each particle type, we carried out several RH cycles or experiments. For aqueous ammonium sulfate droplets without solid material, three cycles were carried out for a total of 172 droplets. For aqueous ammonium sulfate droplets with *n*-hexane soot, six cycles were performed for a total of 350 droplets. For aqueous ammonium sulfate droplets with kaolinite, six cycles were performed for a total of 225 droplets. The results from all these measurements are summarized in Figure 3, panel A. This figure takes into account particle size and, hence, can be used to compare directly the results from the different particle types. In Figure 3, panel A, we have plotted, as a function of droplet diameter, the RH at which 50% of the particles crystallized (i.e., the median), which we refer to as CRH50. Figure 3, panel A, was generated by sorting the crystallization data into bins according to the particle size (with a bin width of about 3 μm over the range of 5−25 μm, and a bin width of 5 μm over the range of 25−30 μm). Then for each bin, the CRH50 was calculated if the number of nucleation events in the bin was greater than 5. The symbols in Figure 3, panel A, correspond to CRH50 values at the average diameter for each size bin and the vertical bars indicate the 20th and 80th percentiles of the

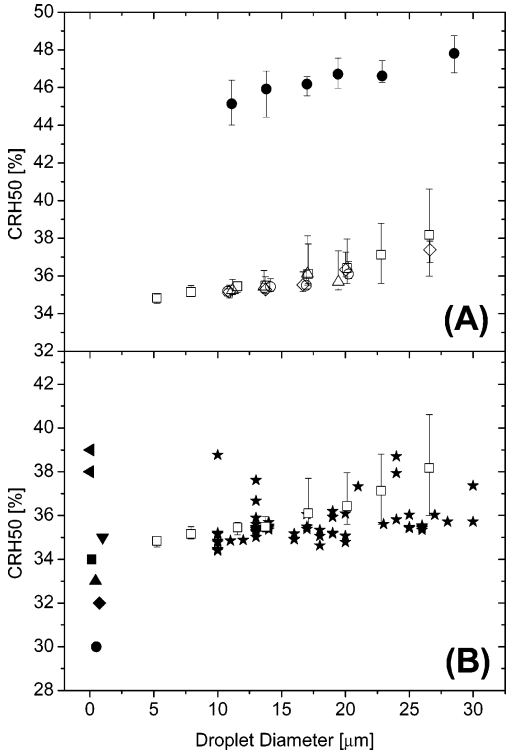

Figure 3. (A) CRH50 as a function of aqueous droplet diameter for the current data and (B) comparison of current CRH50 data for aqueous ammonium sulfate droplets free of solid material with crystallization RH data from previous studies. Key: aqueous ammonium sulfate: (□) current data; (▼) ref 19; (■) ref 47; (●) ref 48; (▲) ref 49; (◆) ref 50; (triangle pointing left) ref 51; (★) ref 52; aqueous ammonium sulfate internally mixed with: (○) *n*-hexane soot current data (diffusion flame); (◇) *n*-hexane soot current data (air:fuel = 0.53); (△) *n*-hexane soot current data (Air: Fuel = 2.4); (●) kaolinite current data. The vertical bars indicate the 20th and 80th percentiles of the crystallization RH data in each particle size bin.

crystallization RH data in each size bin. This method of presenting our crystallization data is similar to that of Koop et al.[46]

For pure ammonium sulfate (open squares in Figure 3) the CRH50 ranges from 35 to 38% RH depending on particle size. In Figure 3, panel B, we compare the current results for aqueous ammonium sulfate free of solid material with results from the literature using submicrometer particles[19,47−51] and our previous size dependent measurements, which utilized an electrodynamic trap and supermicrometer particles.[52] Our results are in good agreement with most of these previous studies. On the basis of this, we suggest the crystallization of pure ammonium sulfate is not significantly affected by the presence of the PTFE surface supporting the particles in our experiments. Furthermore, the results in Figure 3 show that the crystallization RH does not change significantly with particle size. This is consistent with conclusions made previously in the literature based on comparisons of results from different laboratories, (see, for example, refs 2, 19, 23, and 47−51) and also a recent detailed study of the effect of particle size on crystallization carried out in our laboratory with an electrodynamic balance.[52]

Figure 3, panel A, shows that the crystallization results for aqueous ammonium sulfate droplets containing soot (with a mass ratio of soot to ammonium sulfate equal to 0.01) are statistically equivalent to the results for aqueous ammonium sulfate droplets with no solid particulates. This indicates that *n*-hexane soot is not an effective nucleus for crystallization of ammonium sulfate. As mentioned in the Introduction, the effects of soot or carbon black on the crystallization of aqueous inorganic droplets have been investigated in two other studies. Dougle et al.[17] found that the addition of soot from the combustion of diesel fuel did not influence crystallization of aqueous ammonium nitrate droplets or aqueous droplets consisting of 2:1 internal mixtures by weight of ammonium nitrate to ammonium sulfate. Also, Even et al.[18] found that Talens Indian ink (a type of carbon black) did not influence the crystallization of aqueous sodium chloride droplets. Our results give further support that soot does not influence the crystallization of aqueous inorganic droplets.

Figure 3, panel A, also shows that kaolinite (with a mass ratio of kaolinite to ammonium sulfate equal to 0.01) does induce crystallization of ammonium sulfate, increasing the CRH50 values by approximately 10% from those of the aqueous ammonium sulfate droplets with no solid particulates. Also the CRH50 increases slightly as the droplet size increases. This is because the larger droplets have a larger surface area available for heterogeneous nucleation. This study is the first to investigate the effect of kaolinite on the crystallization RH of aqueous ammonium sulfate droplets. Others have investigated the effect of other types of solid inorganic material on the crystallization RH of aqueous ammonium sulfate droplets.[19,21−23] The results from these other studies as well as our result for kaolinite are summarized in Table 2. Comparing the crystallization RH values in Table 2, it is clear that some solid inorganic materials act as better heterogeneous nuclei than others. For example, it appears that Al_2O_3, ZrO_3, and TiO_3 are significantly better heterogeneous nuclei than kaolinite as the crystallization RH values are higher for these inorganic solids compared with kaolinite crystallization RH values, despite the fact that the surface area available for heterogeneous nucleation per droplet was lower in these previous experiments compared with our kaolinite experiments. (Note, to compare results from different experiments the difference in surface area should be considered. This is discussed in more detail below.)

3.2. Nucleation Rates from Experimental Data. From the crystallization results discussed above, we determine the homogeneous nucleation rates of crystalline ammonium sulfate in aqueous ammonium sulfate droplets (free of solid material) and the heterogeneous nucleation rates of crystalline ammonium sulfate in aqueous ammonium sulfate droplets containing kaolinite. A similar analysis was not performed for aqueous ammonium sulfate droplets containing soot since soot did not significantly influence the crystallization RH of the aqueous ammonium sulfate droplets. In sections 3.3 and 3.4 the nucleation rates are parameterized using classical nucleation theory, and the parameters from this analysis are used in section 4 to predict the impact of kaolinite on the crystallization RH of aqueous ammonium sulfate particles in the atmosphere.

From the data for aqueous ammonium sulfate droplets without solid material, we calculated the homogeneous nucleation rate, J_{hom}, which is the number of nucleation events per unit volume of aqueous solution per unit time. Note this is also often referred to as the homogeneous nucleation rate constant in the atmospheric literature. J_{hom} can be calculated with following equation:[2,52,53]

$$J_{hom}(RH) = -\frac{r}{VN(RH)}\frac{dN(RH)}{dRH} \quad (1)$$

where N(RH) is the total number of liquid droplets (not including droplets that have crystallized), and the product VN(RH) is the total volume of liquid droplets (again, not including droplets that have crystallized), dN(RH) is the number of droplets

TABLE 2: Comparison of Measurements of the Crystallization RH of Aqueous Ammonium Sulfate Droplets Containing Inorganic Solids

solid inclusion	temp (K)	crystallization RH (% RH)	surface area of solid inclusion per droplet (m^2)	observation time (s)	ref
none	293.2	34.3 ± 1 to 42.5 ± 1	0	~120	current study
kaolinite	293.2	42.4 ± 1 to 50.1 ± 1	$(0.8-20) \times 10^{-10}$	~120	current study
Al_2O_3	298	57	8×10^{-13}	120	19
ZrO_3	298	59	8×10^{-13}	120	19
TiO_2	298	65	8×10^{-13}	120	19
hematite	298	35−59	$(0.1-6) \times 10^{-13}$	120	21
corundum	298	33−53	$(0.1-3) \times 10^{-13}$	120	21
mullite	298	43	2×10^{-13}	120	21
amorphous silica	298	35	2×10^{-13}	120	21
$BaSO_4$	298	45.8	3×10^{-14}	≤1	22
$CaCO_3$	298	48.5	2×10^{-13}	≤1	22
$CaCO_3$	298	46.6−49.4	$(8-10) \times 10^{-13}$	≤1	23

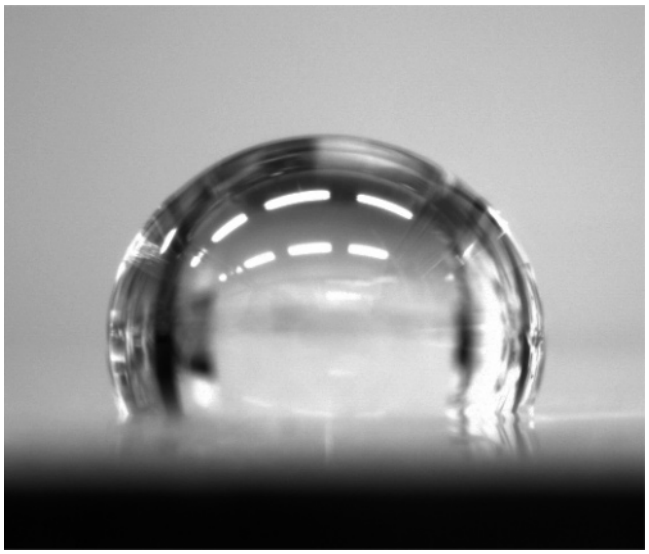

Figure 4. Side view of an aqueous ammonium sulfate solution droplet on a PTFE substrate. The contact angle of the droplet on the PTFE substrate was about 120° for all systems studied.

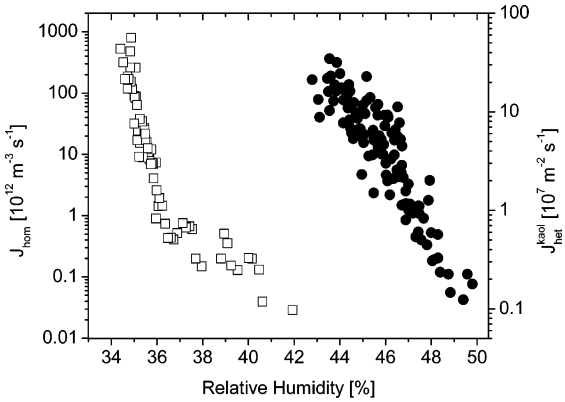

Figure 5. Nucleation rates as a function of relative humidity. The open squares correspond to the nucleation rates (J_{hom}) of solid ammonium sulfate in aqueous ammonium sulfate droplets determined in this study (corresponding to the left ordinate). The solid circles correspond to nucleation rates (J_{het}^{kaol}) of solid ammonium sulfate in aqueous ammonium sulfate droplets containing kaolinite (corresponding to the right ordinate).

observed to crystallize between RH and (RH − dRH), and r is the rate of change of the RH, which is −0.5% RH min^{-1} in these experiments. Equation 1 assumes that the rate limiting step for crystallization is nucleation of the solute and that only one nucleation event leads to the solidification of the droplet, which is a reasonable assumption for our conditions. Equation 1 also assumes that crystallization is dominated by homogeneous nucleation rather than heterogeneous nucleation by foreign nuclei or heterogeneous nucleation on the PTFE substrate supporting the particles. We calculated dN(RH)/dRH by first plotting N vs RH (the plot is similar to Figure 2 except that the total number of liquid droplets, N, is plotted instead of fraction liquid). Then at each RH measurement, we calculated dN(RH)/dRH by the central difference approximation, which is a numerical method for differentiation. VN(RH) was determined by summing the volume of all the liquid droplets (not including droplets that have crystallized) at each crystallization RH measurement. The volume of each droplet was calculated from the droplet diameter immediately before crystallization and the contact angle between aqueous ammonium sulfate droplets and the PTFE surface. Shown in Figure 4 is an image of an aqueous ammonium sulfate droplet on the PTFE surface prior to crystallization, recorded with a CCD camera coupled to a microscope held in the same plane as the PTFE surface. As mentioned above the contact angle between aqueous ammonium sulfate droplets and the PTFE surface was close to 120°, and this angle does not change significantly with droplet composition or over the range of RH values investigated in these experiments. When calculating the volume of the droplets, we took into account the fact that the droplets form a spherical cap (i.e., a sphere truncated by a plane) on the PTFE surface. From dN(RH)/dRH and VN(RH) we determine J_{hom} using eq 1. Shown in Figure 5 is a plot of J_{hom} vs RH for pure ammonium sulfate droplets, calculated using eq 1 and our crystallization results. Note that J_{hom} (which has units of m^{-3} s^{-1}) corresponds to the left ordinate in Figure 5.

From our crystallization data for aqueous ammonium sulfate droplets internally mixed with kaolinite, we calculated the heterogeneous nucleation rate on kaolinite, J_{het}^{kaol}, which we define as the number of nucleation events of crystalline ammonium sulfate per unit surface area of solid kaolinite per unit time. J_{het}^{kaol} can be described with the following equation:

$$J_{het}^{kaol}(\mathrm{RH}) = -\frac{r(\mathrm{RH})}{AN(\mathrm{RH})}\frac{\mathrm{d}N(\mathrm{RH})}{\mathrm{dRH}} \qquad (2)$$

The surface area of kaolinite per liquid droplet, A, was calculated from knowledge of the BET surface area per unit mass of the kaolinite material, the volume of the aqueous droplet (taking into account the spherical cap geometry), and the composition of the aqueous droplets as a function of RH, which can be determined from the model by Clegg et al.[54,55] AN(RH) corresponds to the total surface area (of kaolinite) available for

heterogeneous nucleation in the experiments (not including the surface area of kaolinite in droplets that have crystallized). J_{het}^{kaol} is determined with a method similar to the method used to determine J_{hom} (see above) except *AN*(RH) is used in place of *VN*(RH). It should be noted that eq 2 applies only when heterogeneous nucleation dominates over homogeneous nucleation, which is the case under our experimental conditions.

Shown in Figure 5 is a plot of J_{het}^{kaol} as a function of RH calculated with eq 2 and our experimental results. Note that J_{het}^{kaol} (which has units of m^{-2} s^{-1}) corresponds to the right ordinate in Figure 5.

3.3. Classical Nucleation Theory Parameters from J_{hom}. From the homogeneous nucleation rates calculated above, we determined the interfacial tension between an ammonium sulfate critical nucleus and an aqueous ammonium sulfate solution. According to classical nucleation theory the homogeneous nucleation rate, J_{hom}, can be described by the following equation:[56]

$$J_{hom} = \alpha_{hom} \exp\left(-\frac{\Delta G_{hom}^{crit} + \Delta G'}{kT}\right) \quad (3)$$

where α_{hom} is a preexponential factor, T is the temperature, k is the Boltzmann constant, ΔG_{hom}^{crit} is the free energy of formation of a critical nucleus, and $\Delta G'$ is the activation energy for molecular motion across the embryo-matrix interface.[56] Assuming a spherical critical nucleus, the free energy of formation of a critical nucleus is given by[56]

$$\Delta G_{hom}^{crit} = \frac{16\pi\gamma^3\nu^2}{3(kT \ln S)^2} \quad (4)$$

where γ is the interfacial tension between the crystalline ammonium sulfate critical nucleus and an aqueous ammonium sulfate solution, ν is the molecular volume (124 Å^3 for ammonium sulfate[57]), T is the temperature, and S is the supersaturation defined as

$$S = \frac{a_{solute}}{a_{solute}^{sat}} \quad (5)$$

where a_{solute} is the activity of the solute, and a_{solute}^{sat} is the activity of solute in a saturated solution. Combining eqs 3 and 4 gives the following

$$J_{hom} = J_{0,hom} \exp\left(-\frac{16\pi\gamma^3\nu^2}{3k^3T^3(\ln S)^2}\right) \quad (6)$$

where

$$J_{0,hom} = \alpha_{hom} \exp\left(-\frac{\Delta G'}{kT}\right) \quad (7)$$

The nucleation rate described by eq 6 exhibits a strong dependence on the supersaturation due to the quantity $(\ln S)^2$ that appears in the exponential term. $J_{0,hom}$ is expected to be relatively insensitive to changes in temperature and supersaturation, at least over a relatively narrow range of these variables.[58−61]

In Figure 6, we have plotted $\ln J_{hom}$ vs $(\ln S)^{-2}$ for aqueous $(NH_4)_2SO_4$ particles. The thermodynamic model by Clegg et al.[54,55] was used to calculate S in the aqueous ammonium sulfate droplets. Note that $\ln J_{hom}$ corresponds to the left ordinate in Figure 6. Interestingly, the $\ln J_{hom}$ data in Figure 6 do not seem to fall perfectly on a straight line. A possible explanation is

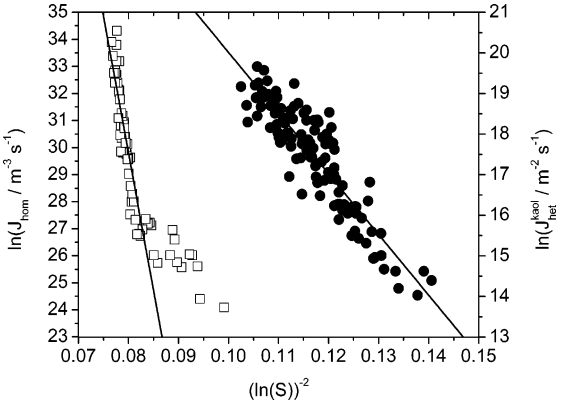

Figure 6. Nucleation results as a function of supersaturation. The open squares correspond to the nucleation rates ($\ln J_{hom}$) of solid ammonium sulfate in aqueous ammonium sulfate droplets (corresponding to the left ordinate). The solid circles correspond to nucleation rates ($\ln J_{het}^{kaol}$) of solid ammonium sulfate in aqueous ammonium sulfate droplets containing solid kaolinite (corresponding to the right ordinate). The lines are linear fits to the data (neglecting the first 13% of crystallization events of aqueous ammonium sulfate droplets without solid material).

that $J_{0,hom}$ or γ vary significantly with a change in S. In the literature, there are many studies where nucleation data also do not fall on a single line when $\ln J_{hom}$ is plotted vs $(\ln S)^{-2}$ (see for example refs 56 and 62−64). Often the data in the literature exhibit two different kinetic regions and the trend is attributed to homogeneous nucleation at high supersaturations and heterogeneous nucleation at low supersaturations. When γ was calculated in these previous studies, only nucleation rates at high supersaturation were considered, and nucleation rates at low supersaturations (which potentially may have been influenced by heterogeneous nucleation) were not included in the analysis.[56,62−64] We follow a similar procedure here.

To determine $\ln J_{0,hom}$ and γ, we neglected the first 13% of the crystallization events. In other words, we neglected all crystallization events that occurred at $(\ln S)^{-2} > 0.085$, or RH values >37.7% RH. A linear fit to the results excluding the first 13% of the crystallization events is included in Figure 6. Over the range of $(\ln S)^{-2} < 0.085$ the data fit well to a straight line when $\ln J_{hom}$ is plotted vs $(\ln S)^{-2}$. The $\ln J_{0,hom}$ and γ values determined from the intercept and slope of this line are given in Table 3. The uncertainties given for $\ln J_{0,hom}$ and γ come from the 95% confidence limits of the intercept and slope from the linear fit. Also included in Table 3 are $\ln J_{0,hom}$ and γ determined in other studies. The parameters determined from Figure 6 are in good agreement (within limits of uncertainty) with the values from Parsons et al.[52] The γ value determined in this study is greater than the γ values determined by Onasch et al.[23] and Mohan et al.[65] This discrepancy is likely due to the assumptions made in calculating γ in these previous studies. Onasch et al.[23] measured the RH at which aqueous particles crystallized and then from an estimate of the induction time and an estimate of $J_{0,hom}$ they calculated a homogeneous nucleation rate (at one RH) and γ. Mohan et al.[65] estimated γ based on a measurement of the spinodal curve concentration. Note that in the work by Parsons et al.[52] two kinetic regions in the experimental data were not clearly discernible. This may be because heterogeneous nucleation by foreign impurities was less of an issue in the previous experiments by Parsons et al.[52] where droplets suspended in an electrodynamic balance were studied.

3.4. Classical Nucleation Theory Parameters from J_{het}^{kaol}. From the heterogeneous nucleation rate on kaolinite (J_{het}^{kaol}) we

TABLE 3: Classical Nucleation Theory Parameters (See Text) for Aqueous Ammonium Sulfate with and without Kaolinite Determined from Experimental Results

parameter	current data	Mohan et al.[65]	Onasch et al.[23]	Parsons et al.[52]
temp (K)	293.2 ± 0.1	298	298	295−300
$\ln(J_{0,\mathrm{hom}}/\mathrm{m}^{-3}\,\mathrm{s}^{-1})$	111 ± 10			74−129
$\ln(J_{0,\mathrm{het}}^{\mathrm{kaol}}/\mathrm{m}^{-2}\,\mathrm{s}^{-1})$	35 ± 2			
γ (J m^{-2})	0.064 ± 0.003	0.05829572	0.052	0.053−0.070
θ (deg)	59 ± 2			

determined the contact angle between an ammonium sulfate critical nucleus and the kaolinite surface. On the basis of classical nucleation theory the heterogeneous nucleation rate on kaolinite can be described with the following equation:[56]

$$J_{\mathrm{het}}^{\mathrm{kaol}} = \alpha_{\mathrm{het}} \exp\left(-\frac{\Delta G_{\mathrm{crit,hom}}\phi + \Delta G'}{kT}\right) \tag{8}$$

Here α_{het} is the preexponential factor for heterogeneous nucleation and ϕ is described by the following equation:[56]

$$\phi = \frac{(2+\cos\theta)(1-\cos\theta)^2}{4} \tag{9}$$

θ is the contact angle between the crystalline critical nucleus and the surface of kaolinite. For convenience, we define $J_{0,\mathrm{het}}^{\mathrm{kaol}}$ as

$$J_{0,\mathrm{het}}^{\mathrm{kaol}} = \alpha_{\mathrm{het}} \exp\left(-\frac{\Delta G'}{kT}\right) \tag{10}$$

The combination of eqs 4 and 8−10 gives an expression for the heterogeneous nucleation rate in terms of the interfacial tension and the contact angle:

$$J_{\mathrm{het}}^{\mathrm{kaol}} = J_{0,\mathrm{het}}^{\mathrm{kaol}} \exp\left(-\frac{16\pi\gamma^3\nu^2}{3k^3T^3(\ln S)^2}\frac{(2+\cos\theta)(1-\cos\theta)^2}{4}\right) \tag{11}$$

In Figure 6, we have plotted $\ln J_{\mathrm{het}}^{\mathrm{kaol}}$ vs $(\ln S)^{-2}$. Note that $\ln J_{\mathrm{het}}^{\mathrm{kaol}}$ corresponds to the right ordinate in Figure 6. A linear fit to the results is included in Figure 6. It appears that the data fit well to a single straight line. From the slope and intercept of $\ln J_{\mathrm{het}}^{\mathrm{kaol}}$ vs $(\ln S)^{-2}$ we determined $\ln J_{0,\mathrm{het}}^{\mathrm{kaol}}$ and θ for kaolinite. These values are given in Table 3. The uncertainties given for $\ln J_{0,\mathrm{het}}^{\mathrm{kaol}}$ and θ come from the 95% confidence limits of the intercept and slope from the linear fit, respectively. Note that we used the γ value determined from the homogeneous nucleation measurements when calculating θ from the slope of the line.

4. Atmospheric Implications

4.1. Atmospheric Implications of the Soot Studies. It is clear from Figure 3 that *n*-hexane soot particles do not influence the crystallization RH under our experimental conditions (observation time and soot surface area). In our experiments the average soot surface area per 30 μm droplet was 4×10^{-8} m^2, according to the average BET surface area per unit mass for *n*-hexane soot given in Table 1. On the basis of data from several field studies, Blake and Kato[66] found that the average diameter of soot particles in the atmosphere is approximately 0.2 μm and they estimated that the average atmospheric soot particle surface area was 4×10^{-12} m^2 (assuming a fractal geometry with the total volume of a soot particle composed of 20 nm spheres). Hence, the average atmospheric soot particle surface area is approximately 4 orders of magnitude less than the surface area used in our experiments. Soot did not influence the crystallization RH values in our experiments, so it is unlikely that soot will influence crystallization of atmospheric aqueous droplets (if the soot particles have the same chemical and physical properties as the soot particles investigated in our studies).

4.2. Atmospheric Implications of the Kaolinite Studies. It is clear from Figure 3 that kaolinite does influence the crystallization RH in our experiments. To put our measurements into an atmospheric context, we calculated the RH at which 50% of aqueous ammonium sulfate droplets internally mixed with kaolinite particulates will crystallize using atmospherically relevant times and kaolinite particulate sizes. We used diameters ranging from 0.1 to 5 μm for atmospherically relevant kaolinite particulate sizes, which is approximately the size range of mineral dust in the atmosphere (see for example, ref 67). Residence times of aerosols in the atmosphere are approximately a week. For this discussion, however, it is more appropriate to consider the temporal variation of RH in the atmosphere. In the continental boundary layer, the RH is often low in the summer and there is a strong diurnal cycle, and the diurnal variation often exhibits a continuously changing relative humidity covering a RH range of typically more than 10%. For these calculations we will assume that the particles are held at a constant RH for approximately 8 h, which is a simplification to the true diurnal variation. We also assume that each aqueous ammonium sulfate droplet is internally mixed with a single kaolinite particulate. Finally we assume that the fraction of aqueous ammonium sulfate droplets crystallized can be calculated with the following equation:

$$F(\mathrm{RH},t) = 1 - \exp[-(J_{\mathrm{het}}^{\mathrm{kaol}}(\mathrm{RH})A + J_{\mathrm{hom}}(\mathrm{RH})V)t] \tag{12}$$

Here $F(\mathrm{RH},t)$ is the fraction of ammonium sulfate particles that have crystallized. This equation is consistent with classical nucleation theory and the statistics of nucleation.[56,68] To calculate the nucleation rate of crystalline ammonium sulfate on kaolinite in aqueous ammonium sulfate droplets, we use the parameters listed in Table 3. Shown in Figure 7 is the RH at which 50% of aqueous ammonium sulfate droplets containing kaolinite will crystallize (i.e., the CRH50) under the conditions mentioned above (i.e., $t = 8$ h). As an example, the CRH50 of aqueous ammonium sulfate droplets with a kaolinite particulate 0.1 μm in diameter will be 41.4 ± 0.5% RH. Note that the CRH50 is independent of the aqueous ammonium sulfate droplet size since heterogeneous nucleation dominates for this size range of kaolinite inclusion. For comparison, the CRH50 of 0.5 μm diameter aqueous ammonium sulfate droplets free of solid material will be 34.3 ± 0.5% RH, assuming an observation time of 8 h, using the parameters in Table 3, and setting A equal to zero in eq 12 to calculate the homogeneous nucleation rate. Also note that Figure 7 suggests that the CRH50 of aqueous ammonium sulfate droplets in the atmosphere will depend strongly on the size of the kaolinite particulate, increasing by

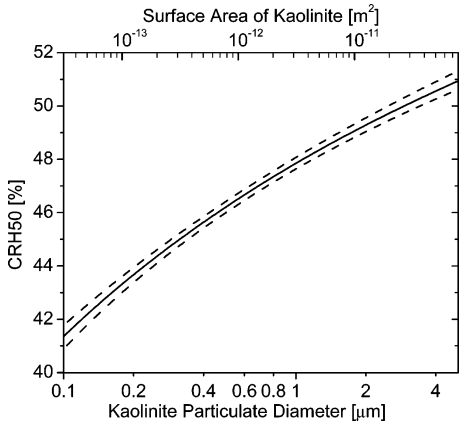

Figure 7. Calculated size of a kaolinite inclusion needed to crystallize 50% (i.e., the CRH50) of the aqueous ammonium sulfate droplets in the atmosphere (solid line). The calculation assumes that every aqueous ammonium sulfate droplet contains a single, spherical kaolinite inclusion and that the relevant time in the atmosphere for crystallization is approximately 8 h, which is a simplification to the diurnal cycle of RH (see text). Calculations were carried out using eq 12 and the parameters listed in Table 3. Dashed lines indicate the uncertainty of the calculation based on the uncertainty of the parameters given in Table 3.

about 6% RH with an increase in the diameter of the kaolinite particulate by 1 order of magnitude or an increase in kaolinite surface area of 2 orders of magnitude. This trend is also observed in our CRH50 data presented in Figure 3, panel A. Based on Figure 3, panel A, the CRH50 for droplets with kaolinite increases by approximately 3% when the kaolinite surface area increases by a factor of 9. (In our experiments, we assume that the surface area of kaolinite per unit volume in the droplets is independent of droplet size, and hence, an increase in volume by a factor of 9 also leads to an increase in surface area of kaolinite by a factor of 9.) This observed increase is consistent with the predictions in Figure 7.

A few caveats to the above discussion should be mentioned at this point. First, kaolinite typically only represents 5 to 10% of the total mass of mineral dust particles in the atmosphere,[67] and the other components of mineral dust may also influence the crystallization RH. To accurately predict the effect of mineral dust on crystallization, the entire composition of the dust needs to be considered. Our work is a starting point for this analysis. Second, we assumed in the above calculations that each aqueous ammonium sulfate droplet is internally mixed with a kaolinite particulate. This, of course, is an upper limit. Equation 12 should only be used to predict the crystallization relative humidity of ammonium sulfate particles that contain kaolinite inclusions (i.e., kaolinite particles with ammonium sulfate coatings); it should not be used to predict the crystallization relative humidity of the entire aerosol population. In regions far removed from large dust sources, a majority of the ammonium sulfate particles will not contain mineral dust, although the majority of the mineral dust particles may contain ammonium sulfate. Third, our analysis assumes that the results can be described by classical nucleation theory. This provided a straightforward method to parametrize our data and extrapolate the results to atmospheric scenarios but suffers from the assumptions inherent to classical nucleation theory. Several others in the past have also used classical nucleation theory to analyze and interpret crystallization results as well as ice nucleation measurements (see for example refs 11, 22−24, 69, and 70). Nevertheless, more work, similar to the work by Martin and colleagues,[19,21,69] is needed to determine the general applicability of classical nucleation theory to the heterogeneous crystallization of atmospheric particles. Results by Martin et al.[21] and Han and Martin[19] show that an active site model is needed to precisely describe nucleation of crystalline ammonium sulfate and ammonium nitrate on hematite and corundum inclusions. Ice nucleation results on mineral dust cores by Hung et al.[69] also showed some deviation from ideal classical nucleation theory, in that smaller particles had a higher surface-normalized nucleation rate. However, the deviation from classical nucleation theory only resulted in a small uncertainty when calculating important variables like average freezing temperatures.[69] Until further information is available, the classical nucleation analysis discussed above provides an initial estimate of the effect of kaolinite on the crystallization of aqueous ammonium sulfate droplets.

5. Conclusions and Summary

Our results show that the crystallization RH of aqueous ammonium sulfate droplets free of solid material does not depend strongly on droplet size, in agreement with our previous work conducted with droplets suspended in an electrodynamic balance.[52] In addition, our results show that soot did not influence the crystallization RH of aqueous ammonium sulfate particles under our experimental conditions (observation time and soot surface area per droplet). In contrast, kaolinite increased the crystallization RH of the aqueous ammonium sulfate droplets by approximately 10% RH.

From the crystallization results, we determined the homogeneous nucleation rates of crystalline ammonium sulfate in aqueous ammonium sulfate droplets and the heterogeneous nucleation rates of crystalline ammonium sulfate in aqueous ammonium sulfate droplets containing kaolinite. In addition, we parametrized these rates using classical nucleation theory. On the basis of this analysis, the interfacial tension between an ammonium sulfate critical nucleus and an aqueous ammonium sulfate solution, γ, is 0.064 ± 0.003 J m^{-2} (in agreement with our previous measurements[52]), and the contact angle between an ammonium sulfate critical nucleus and a kaolinite surface, θ, is $59 \pm 2°$.

Our laboratory results were also used to determine whether soot or kaolinite will influence the crystallization RH of aqueous ammonium sulfate droplets in the atmosphere. On the basis of our results, we argue that soot will not influence the crystallization of aqueous ammonium sulfate particles in the atmosphere. Additionally, using γ determined from our homogeneous measurements and θ determined from our kaolinite measurements, we argue that kaolinite can significantly influence the crystallization of aqueous ammonium sulfate droplets in the atmosphere. As an example, the CRH50 (RH at which 50% of aqueous droplets crystallize) ranges from about 41 to 51% RH when the kaolinite particulate ranges from 0.1 to 5 μm in diameter. For comparison, the CRH50 of aqueous ammonium sulfate droplets (0.5 μm in diameter) free of solid material is approximately 34.3% RH for a common atmospheric scenario. Kaolinite typically represents 5−10% of the total mass of mineral dust particles,[67] and the other components of mineral dust may also influence the crystallization RH. Hence, further research on the other components of mineral dust is needed.

Acknowledgment. The authors thank D. Smith for helpful discussions on the properties of soot as well as for providing samples of *n*-hexane soot. We also thank D. A. Knopf and B. J. Murray for helpful comments on the manuscript. This work was funded by the Natural Science and Engineering Research

Council of Canada, the Canada Foundation for Innovation, and the Canada Research Chair Program.

References and Notes

(1) Finlayson-Pitts, B. J.; Pitts, J. N. *Chemistry of the Upper and Lower Atmosphere: Theory, Experiments and Applications*; Academic Press: San Diego, CA, 2000.
(2) Martin, S. T. *Chem. Rev.* **2000**, *100*, 3403.
(3) Seinfeld, J. H.; Pandis, S. N. *Atmospheric Chemistry and Physics: From Air Pollution to Climate Change*; Wiley: New York, 1998.
(4) Zuberi, B.; Bertram, A. K.; Koop, T.; Molina, L. T.; Molina, M. J. *J. Phys. Chem. A* **2001**, *105*, 6458.
(5) Heintzenberg, J. *Tellus* **1989**, *41B*, 149.
(6) Braban, C. F.; Abbatt, J. P. D. *Atmos. Chem. Phys.* **2004**, *4*, 1451.
(7) Brooks, S. D.; DeMott, P. J.; Kreidenweis, S. M. *Atmos. Environ.* **2004**, *38*, 1859.
(8) Choi, M. Y.; Chan, C. K. *Environ. Sci. Technol.* **2002**, *36*, 2422.
(9) Cruz, C. N.; Pandis, S. N. *Environ. Sci. Technol.* **2000**, *34*, 4313.
(10) Hansson, H.-C.; Rood, M. J.; Koloutsou-Vakakis, S.; Hämeri, K.; Orsini, D.; Wiedensohler, A. *J. Atmos. Chem.* **1998**, *31*, 321.
(11) Lightstone, J. M.; Onasch, T. B.; Imre, D.; Oatis, S. *J. Phys. Chem. A* **2000**, *104*, 9337.
(12) Marcolli, C.; Krieger, U. K. *J. Phys. Chem. A* **2006**, *110*, 1881.
(13) Mikhailov, E.; Vlasenko, S.; Niessner, R.; Pöschl, U. *Atmos. Chem. Phys.* **2004**, *4*, 323.
(14) Pant, A.; Fok, A.; Parsons, M. T.; Mak, J.; Bertram, A. K. *Geophys. Res. Lett.* **2004**, *31*, art. no. L12111, doi: 10.1029/2004GL020025.
(15) Parsons, M. T.; Knopf, D. A.; Bertram, A. K. *J. Phys. Chem. A* **2004**, *108*, 11600.
(16) Prenni, A. J.; DeMott, P. J.; Kreidenweis, S. M. *Atmos. Environ.* **2003**, *37*, 4243.
(17) Dougle, P. G.; Veefkind, J. P.; ten Brink, H. M. *J. Aerosol Sci.* **1998**, *29*, 375.
(18) Even, A.; ten Brink, H. M.; Khlystov, A.; Smekens, A.; Berghmans, P.; van Grieken, R. *J. Aerosol Sci.* **2000**, *31*, S336.
(19) Han, J. H.; Martin, S. T. *J. Geophys. Res.* **1999**, *104*, 3543.
(20) Han, J. H.; Hung, H. M.; Martin, S. T. *J. Geophys. Res.* **2002**, *107*, art. no. 4086, doi: 10.1029/2001JD001054.
(21) Martin, S. T.; Han, J. H.; Hung, H. M. *Geophys. Res. Lett.* **2001**, *28*, 2601.
(22) Oatis, S.; Imre, D.; McGraw, R.; Xu, J. *Geophys. Res. Lett.* **1998**, *25*, 4469.
(23) Onasch, T. B.; McGraw, R.; Imre, D. *J. Phys. Chem. A* **2000**, *104*, 10797.
(24) Richardson, C. B.; Snyder, T. D. *Langmuir* **1994**, *10*, 2462.
(25) Buseck, P. R.; Posfai, M. *P. Natl. Acad. Sci. USA* **1999**, *96*, 3372.
(26) Lee, S. H.; Murphy, D. M.; Thomson, D. S.; Middlebrook, A. M. *J. Geophys. Res.* **2002**, *107*, art. no. 4003, doi: 10.1029/2000JD000011.
(27) Pósfai, M.; Anderson, J. R.; Buseck, P. R.; Sievering, H. *J. Geophys. Res.* **1999**, *104*, 21685.
(28) Vogt, R.; Kirchner, U.; Scheer, V.; Hinz, K. P.; Trimborn, A.; Spengler, B. *J. Aerosol Sci.* **2003**, *34*, 319.
(29) Andreae, M. O.; Charlson, R. J.; Bruynseels, F.; Storms, H.; Vangrieken, R.; Maenhaut, W. *Science* **1986**, *232*, 1620.
(30) Laskin, A.; Iedema, M. J.; Ichkovich, A.; Graber, E. R.; Taraniuk, I.; Rudich, Y. *Faraday Discuss.* **2005**, *130*, 453.
(31) Laskin, A.; Wietsma, T. W.; Krueger, B. J.; Grassian, V. H. *J. Geophys. Res.* **2005**, *110*, art. no. D10208, doi: 10.1029/2004JD005206.
(32) Liu, D. Y.; Wenzel, R. J.; Prather, K. A. *J. Geophys. Res.* **2003**, *108*, art. no. 8426, doi: 10.1029/2001JD001562.
(33) Murphy, D. M.; Thomson, D. S. *J. Geophys. Res.* **1997**, *102*, 6353.
(34) Glaccum, R. A.; Prospero, J. M. *Mar. Geol.* **1980**, *37*, 295.
(35) Pye, K. *Aeolian Dust and Dust Deposits*; Academic Press: London; Orlando, 1987.
(36) Perry, K. D.; Cahill, T. A.; Eldred, R. A.; Dutcher, D. D.; Gill, T. E. *J. Geophys. Res.* **1997**, *102*, 11225.
(37) Prospero, J. M. Saharan Dust Transport over the North Atlantic Ocean and Mediterranean: An Overview. In *The Impact of Desert Dust across the Mediterranean*; Guerzoni, S., Chester, R., Eds.; Kluwer Academic Publisher: Dordrecht; Boston, MA, 1996; pp 133−152.
(38) Pósfai, M.; Anderson, J. R.; Buseck, P. R.; Shattuck, T. W.; Tindale, N. W. *Atmos. Environ.* **1994**, *28*, 1747.
(39) Cantrell, W.; Heymsfield, A. *B. Am. Meteorol. Soc.* **2005**, *86*, 795.
(40) DeMott, P. J. Laboratory Studies of Cirrus Cloud Processes. In *Cirrus*; Lynch, D. K., Sassen, K., Starr, D. O'C., Stephens, G., Eds.; Oxford University Press: Cambridge, U.K., and New York, 2002; pp 102−135.
(41) Dentener, F. J.; Carmichael, G. R.; Zhang, Y.; Lelieveld, J.; Crutzen, P. J. *J. Geophys. Res.* **1996**, *101*, 22869.
(42) Dymarska, M.; Murray, B. J.; Sun, L. M.; Eastwood, M. L.; Knopf, D. A.; Bertram, A. K. *J. Geophys. Res.* **2006**, *111*, art. no. D04204, doi: 10.1029/2005JD006627.
(43) Parsons, M. T.; Mak, J.; Lipetz, S. R.; Bertram, A. K. *J. Geophys. Res.* **2004**, *109*, art. no. D06212, doi: 10.1029/2003JD004075.
(44) Chughtai, A. R.; Kim, J. M.; Smith, D. M. *J. Atmos. Chem.* **2002**, *43*, 21.
(45) Akhter, M. S.; Chughtai, A. R.; Smith, D. M. *Appl. Spectrosc.* **1985**, *39*, 143.
(46) Koop, T.; Ng, H. P.; Molina, L. T.; Molina, M. J. *J. Phys. Chem. A* **1998**, *102*, 8924.
(47) Badger, C. L.; George, I.; Griffiths, P. T.; Braban, C. F.; Cox, R. A.; Abbatt, J. P. D. *Atmos. Chem. Phys.* **2006**, *6*, 755.
(48) Brooks, S. D.; Garland, R. M.; Wise, M. E.; Prenni, A. J.; Cushing, M.; Hewitt, E.; Tolbert, M. A. *J. Geophys. Res.* **2003**, *108*, art. no. 4487, doi: 10.1029/2002JD003204.
(49) Cziczo, D. J.; Nowak, J. B.; Hu, J. H.; Abbatt, J. P. D. *J. Geophys. Res.* **1997**, *102*, 18843.
(50) Onasch, T. B.; Siefert, R. L.; Brooks, S. D.; Prenni, A. J.; Murray, B.; Wilson, M. A.; Tolbert, M. A. *J. Geophys. Res.* **1999**, *104*, 21317.
(51) Orr, C.; Hurd, F. K.; Hendrix, W. P. *J. Meteorol.* **1958**, *15*, 240.
(52) Parsons, M. T.; Riffell, J. L.; Bertram, A. K. *J. Phys. Chem. A* **2006**, in press.
(53) Vali, G. *J. Atmos. Sci.* **1994**, *51*, 1843.
(54) Clegg, S. L.; Brimblecombe, P.; Wexler, A. S. *J. Phys. Chem. A* **1998**, *102*, 2137.
(55) Clegg, S. L.; Brimblecombe, P.; Wexler, A. S. Aerosol Inorganics Model. URL: http://www.hpc1.uea.ac.uk/~e770/aim.html, 2002.
(56) Mullin, J. W. *Crystallization*, 4th ed.; Butterworth-Heinemann: Oxford, U.K., and Boston, MA, 2001.
(57) Spann, J. F.; Richardson, C. B. *Atmos. Environ.* **1985**, *19*, 819.
(58) Granberg, R. A.; Ducreux, C.; Gracin, S.; Rasmuson, A. C. *Chem. Eng. Sci.* **2001**, *56*, 2305.
(59) Kashchiev, D. Nucleation. In *Science and Technology of Crystal Growth*; van der Eerden, J. P., Bruinsma, O. S. L., Eds.; Kluwer Academic Publishers: Amsterdam, 1995; pp 53−66.
(60) Mullin, J. W.; Osman, M. M. *Krist. Tech.* **1973**, *8*, 471.
(61) Walton, A. G. Nucleation in Liquids and Solids. In *Nucleation*; Zettlemoyer, A. C., Ed.; M. Dekker: New York, 1969; pp 225−327.
(62) Hendriksen, B. A.; Grant, D. J. W. *J. Cryst. Growth* **1995**, *156*, 252.
(63) Mullin, J. W.; Ang, H. M. *Faraday Discuss.* **1976**, *61*, 141.
(64) Söhnel, O.; Mullin, J. W. *J. Cryst. Growth* **1978**, *44*, 377.
(65) Mohan, R.; Kaytancioglu, O.; Myerson, A. S. *J. Cryst. Growth* **2000**, *217*, 393.
(66) Blake, D. F.; Kato, K. *J. Geophys. Res.* **1995**, *100*, 7195.
(67) Usher, C. R.; Michel, A. E.; Grassian, V. H. *Chem. Rev.* **2003**, *103*, 4883.
(68) Koop, T.; Luo, B. P.; Biermann, U. M.; Crutzen, P. J.; Peter, T. *J. Phys. Chem. A* **1997**, *101*, 1117.
(69) Hung, H. M.; Malinowski, A.; Martin, S. T. *J. Phys. Chem. A* **2003**, *107*, 1296.
(70) Tang, I. N.; Munkelwitz, H. R. *J. Colloid Interface Sci.* **1984**, *98*, 430.